Compressed Sensing Based Joint Sparse Channel Estimation for RIS-Assisted Internet of Things

Zhen Chen
School of Electronic and Information Engineering
Shenzhen University
Shenzhen, China
Chenz.scut@gmail.com

Xiaoyu Du
School of Electronic and Information Engineering
South China University of Technology
Guangzhou, China
dxy293953@163.com

Long Chen
School of Mechanical Engineering
Northwestern Polytechnical University
Xian, China
College of Electronicsand Information Engineering
Shenzhen University,
Shenzhen, China
chenmf767@foxmail.com

***Abstract*—Reconfigurable intelligent surface (RIS) is deemed as a potential technique for the future of the Internet of Things (IoT) due to its capability of tacking the complex propagation environment using a large number of low-cost passive elements. To benefit from RIS technology, the problem of RIS-assisted channel state information (CSI) acquisition needs to be carefully considered. However, existing channel estimation methods usually incorporated line-of-sigh (LOS) channel into reflected channel together, which is not practical for deploying IoT scenarios. In this paper, we study a RIS-aided channel estimation that jointly exploits the properties of the LOS and reflected channels to provide more accurate CSI. The cascaded RIS channel is modeled based upon the weighted ℓ_1 norm minimization, while a LOS channel is exploited using ℓ_1 norm minimization to sequentially estimate the channel parameters. Moreover, by exploiting gradient descent and the alternating minimization method, a flexible and fast algorithm is developed to provide the feasible solution. Simulation results demonstrate that a RIS-aided MIMO system significantly reduces the active antennas/RF chains compared to other benchmark schemes.**

Keywords—channel estimation, compressed sensing, reconfigurable intelligent surface, mmWave MIMO.

I. INTRODUCTION

In the era of the Internet of Things (IoT), the large physical size of antenna array has significantly improved the rate of wireless networks to serve multiple single-antenna IoT devices simultaneously [1][2]. However, the hardware costs and high power consumption are quite challenging in the practical implementations, which will inevitably aggravate the coverage issue for IoT communications. To tackle these challenges, reconfigurable intelligent surface (RIS) is lately gaining increasing interest as a candidate technology to enhance the spectral efficiency (SE) of the fifth generation (5G) networks. The RIS is generally composed of a great number of hardware-efficient passive elements [3], [4], e.g., phase shifters, which can dynamically modify the propagation direction of the incident signal by adjusting its phase shifters, and effectively improve propagation environment with almost negligible power consumption. It is worth mentioning that RIS can also be utilized to bypass some barriers on the channel, or avoid the signal to be monitored. Due to its cost-effective, low-cost hardware and ease of placing, RIS is recognized as one of the key enablers of the IoT vision, which has become a hot spot in the field of communications.

The promising gains brought by RIS are closely dependent on the accuracy of the acquired channel state information (CSI), so channel estimation methods with higher accuracy and lower complexity of are crucial. In [5], by taking advantages of hybrid evolutionary algorithm, compressed sensing (CS)-based channel estimator is derived in RIS-assisted system. Also, in [6], a low-complexity passive beamforming design for the RISs was proposed, but only a large antenna array can achieve satisfied channel estimation. By utilizing the CS-based dictionary learning method, a two-stage channel is estimated for RIS-assisted time-division duplexing system [7]. Subsequently, the sparse structure of RIS channel was applied to the actual system, and the introduction of the sparse channel model and CS stimulated many corresponding optimization schemes and algorithms [8]. By exploring the properties of Kronecker products and the sparsity of RIS channel, the cascaded channel estimation was formulated as a sparse signal recovery problem [9]. To reduce the estimation delay, the author utilizes CS and offset learning, recovering the full channel sensed at few active elements [10]. On basis of this analysis, deep learning (DL)-

based residual learning was exploited to tackle intractable channel optimization problem [11]. The above-mentioned works on channel estimation are limited in hybrid RIS-assisted channel, in which the reflected and LOS channels are estimated together. However, the reflected channels are different from the LOS the channels due to the different path loss exponents between the reflected and LOS pathes. Therefore, it is not applicable to the practical loT scenario.

Motivated by the above problems, this paper proposes a RIS-assisted joint sparse channel estimation for the mmWave Multiple-Input Multiple-Output (MIMO) system by leveraging the properties of the reflected and LOS channels. Specifically, we model the channel estimation of RIS-assist MIMO system as a sparse recovery problem, in which the estimated channel parameters consist of the LOS and reflected paths, in which the channel estimation framework is separated into three separated subproblems by employing the properties of the Kronecker products. Considering the effects of the LOS and reflected channels, the LOS channel estimation based on the weighted ℓ_1 norm minimization is addressed, while the $\ell_{1,\tau}$ norm minimization is formulated to tackle the reflected channel problem. To reduce the training time, a joint channel estimator of weighted ℓ_1 and $\ell_{1,\tau}$ norm is developed by exploiting CS theory. To facilitate the channel estimation, an alternate iteration algorithm is proposed to estimate the reflect-path and LOS path. Simulation results verify the superiorities of the proposed scheme compared with the conventional RIS assisted scheme.

We use the following notations in our paper. Lower case bold font and upper case bold font is used to denote vectors and matrices, respectively. For a vector $\boldsymbol{a}$, $(a)^T$ and $(a)^H$ refer to the transpose, and the conjugate transpose, respectively; $\mathrm{diag}(\cdot)$ is the diagonalization operation. $\tanh(\cdot)$ and $\cosh(\cdot)$ denote hyperbolic tangent and hyperbolic cosine function, respectively. The Euclidean norm of a complex vector is denoted by $\|\cdot\|$. $\mathrm{arctanh}(\cdot)$ inverse hyperbolic tangent function $\nabla_{\mathbf{x}} f(\mathbf{x})$ represents the gradient vector with respect to $\mathbf{x}$. $|\cdot|$ denotes the absolute value of a complex scalar. Symbol $\otimes$ stands for the Kronecker product operator.

II. System Model

Consider a RIS-assisted mmWave MIMO system as shown in Figure 1, where RIS with N_{RIS} reflecting elements is deployed to assist communication. The BS is equipped with N antennas and serves users with M antennas. $\boldsymbol{H}_{BU} \in \mathbb{C}^{M\times N}$ is defined as LOS channel of BS-user link, which can be estimated by traditional method. After RIS power is turned off, the BS-User channel model can be represented as $\boldsymbol{H}_{BU}$. Defining $\boldsymbol{H}_{BRU} \in \mathbb{C}^{M\times N}$ as the channel frequency response of BS-RIS-user cascade link. Therefore, the channel $\boldsymbol{H}$ composed of LoS channel and cascade channel is expressed as

Fig. 1. The RIS-assisted downlink mmWave MIMO system.

$$\begin{aligned}\boldsymbol{H} &= \boldsymbol{H}_{BRU} + \boldsymbol{H}_{BU} \\ &= \boldsymbol{H}_{BR}\boldsymbol{\Phi}\boldsymbol{H}_{RU} + \boldsymbol{H}_{BU},\end{aligned} \tag{1}$$

where $\boldsymbol{H}_{BR}$ and $\boldsymbol{H}_{RU}$ are the channel matrix associated with BS-RIS link and RIS-user link respectively, and $\boldsymbol{\Phi} = \mathrm{diag}\{\varphi_1, \ldots, \varphi_{N_{RIS}}\}$, $\left(\varphi_n = e^{j\theta_n}, n \in \{1, \ldots, N_{RIS}\}\right)$ is the diagonal matrix representing the operation of the RIS. Specifically, θ_n is the phase shift introduced by the n-th element of RIS.

By using the sparse scattering characteristics of mmWave channel, the optimization problem can be expressed as the sparse recovery problem, that is, the channel estimation problem involves finding a sparse geometric channel model, which is characterized by [12]

$$\boldsymbol{H}_{BU} = \sum_{l=1}^{\tilde{L}_{BU}} \alpha_l \boldsymbol{\alpha}_{BS}(\theta_l)\boldsymbol{\alpha}_{UE}^H(\phi_l), \tag{2a}$$

$$\boldsymbol{H}_{BR} = \sum_{l=1}^{\tilde{L}_{BR}} \beta_l \boldsymbol{\alpha}_{BS}(\theta_l)\boldsymbol{\alpha}_{RIS}^H(\psi_l), \tag{2b}$$

$$\boldsymbol{H}_{RU} = \sum_{l=1}^{\tilde{L}_{RU}} \delta_l \boldsymbol{\alpha}_{RIS}(\psi_l)\boldsymbol{\alpha}_{UE}^H(\phi_l), \tag{2c}$$

where $\tilde{L}_{BU}$, $\tilde{L}_{BR}$ and $\tilde{L}_{RU}$ are the path numbers of BS-UE, BS-RIS and RIS-UE respectively. α_l, β_l and δ_l are the l-th path of the complex gain, $\theta_l, \phi_l \in [0, 2\pi]$ are the l-th propagation path of the related AoD and AoA, and $\alpha_{BS} \in \mathbb{C}^{N_{BS}}$ $\left(\alpha_{UE} \in \mathbb{C}^{N_{UE}}, \alpha_{RIS} \in \mathbb{C}^{N_{RIS}}\right)$ are the array response vectors related to BS, UE and RIS, respectively. Suppose uniform linear array (ULA) antenna array is adopted, then the steering vectors at BS, UE and RIS are respectively

$$\boldsymbol{\alpha}_{BS}\left(\theta_l\right)=\frac{1}{\sqrt{N_{BS}}}\left[1,e^{j\frac{2\pi}{\lambda}d\sin\left(\theta_l\right)},\ldots,e^{j\left(N_{BS}-1\right)\frac{2\pi}{\lambda}d\sin\left(\theta_l\right)}\right]^T \tag{3a}$$

$$\boldsymbol{\alpha}_{UE}\left(\phi_l\right)=\frac{1}{\sqrt{N_{UE}}}\left[1,e^{j\frac{2\pi}{\lambda}d\sin\left(\phi_l\right)},\ldots,e^{j\left(N_{UE}-1\right)\frac{2\pi}{\lambda}d\sin\left(\phi_l\right)}\right]^T \tag{3b}$$

$$\boldsymbol{\alpha}_{RIS}\left(\psi_l\right)=\frac{1}{\sqrt{N_{RIS}}}\left[1,e^{j\frac{2\pi}{\lambda}d\sin\left(\psi_l\right)},\ldots,e^{j\left(N_{RIS}-1\right)\frac{2\pi}{\lambda}d\sin\left(\psi_l\right)}\right]^T \tag{3c}$$

where λ is the wavelength of the carrier frequency, and d is the distance between neighboring antenna spacing.

In order to express channel estimation as a sparse signal recovery problem, the LOS channel of RIS-assisted system is

$$\boldsymbol{H}_{BU}=\mathbf{A}_{BS}\boldsymbol{H}_{\alpha}\mathbf{A}_{UE}^{H}, \tag{4}$$

where $\mathbf{A}_{BS}$ and $\mathbf{A}_{UE}$ is the array response matrixs, which can be expressed as

$$\mathbf{A}_{BS}\triangleq\left[\boldsymbol{\alpha}_{BS}\left(\theta_1\right),\ldots,\boldsymbol{\alpha}_{BS}\left(\theta_{L_{BR}}\right)\right], \tag{5a}$$

$$\mathbf{A}_{UE}\triangleq\left[\boldsymbol{\alpha}_{UE}\left(\phi_1\right),\ldots,\boldsymbol{\alpha}_{UE}\left(\phi_{L_{RU}}\right)\right], \tag{5b}$$

$$\mathbf{A}_{RIS}\triangleq\left[\boldsymbol{\alpha}_{RIS}\left(\phi_1\right),\ldots,\boldsymbol{\alpha}_{RIS}\left(\phi_{L_{RIS}}\right)\right] \tag{5c}$$

where $\boldsymbol{H}_{\alpha}\in\mathbb{C}^{N_1\times N_2}$ is the angular domain sparse matrix with $\tilde{L}$ non-zero terms correspond to the channel path gain $\{\alpha_l\}$. Similarly, the following equation exists

$$\boldsymbol{H}_{BR}=\mathbf{A}_{BS}\boldsymbol{H}_{\beta}\mathbf{A}_{RIS}^{H}, \tag{6a}$$

$$\boldsymbol{H}_{RU}=\mathbf{A}_{RIS}\boldsymbol{H}_{\delta}\mathbf{A}_{UE}^{H}, \tag{6b}$$

where $\boldsymbol{H}_{\beta}\in\mathbb{C}^{N_{\delta_1}\times N_{\delta_2}}$ and $\boldsymbol{H}_{\delta}\in\mathbb{C}^{N_{\delta_1}\times N_{\delta_2}}$ are sparse matrices corresponding to the transmission path gains $\{\beta_l\}_{l=1}^{\tilde{L}_{BR}}$ and $\{\delta_l\}_{l=1}^{\tilde{L}_{BR}}$ respectively.

The transmitter uses an active transmitting precoder $\boldsymbol{f}(t)$ to transmit the signal $s(t)$ and combines all receivers with the corresponding receiver precoder $\mathbf{z}(t)$. Therefore, the combined signal $y(t)$ at the receiver can be written as

$$y(t)=\mathbf{z}^H(t)\boldsymbol{H}\boldsymbol{f}(t)s(t)+n(t),\forall t=1,\ldots,T, \tag{7}$$

where $\boldsymbol{H}\in\mathbb{C}^{M\times N}$ is cascade channel matrix, $n(t)$ is additive Gaussian noise. Without losing generality, the pilot signal is set as $s(t)=1$ in the training stage. The noise version of $\mathbf{z}^H\boldsymbol{H}\boldsymbol{f}$ observed by the receiver rather than the direct $\boldsymbol{H}$ limits the application of channel subspace sampling and presents a great challenge to channel estimation.

According to (4), (5) and (6), the received symbol can be represented as follows

$$\begin{aligned}
y(t)&=\left(\boldsymbol{f}^T(t)\otimes\mathbf{z}^H(t)\right)\mathrm{vec}(\boldsymbol{H})+n(t)\\
&\overset{(a)}{=}\left(\boldsymbol{f}^T(t)\otimes\mathbf{z}^H(t)\right)\left(\mathbf{A}_{UE}^{*}\otimes\mathbf{A}_{BS}\right)\boldsymbol{h}_{BU}\\
&\quad+\left(\boldsymbol{f}^T(t)\otimes\mathbf{z}^H(t)\right)\mathrm{vec}\left(\boldsymbol{H}_{BR}\boldsymbol{\Phi}\boldsymbol{H}_{RU}\right)+n(t)\\
&=\left(\boldsymbol{f}^T(t)\otimes\mathbf{z}^H(t)\right)\left(\mathbf{A}_{UE}^{*}\otimes\mathbf{A}_{BS}\right)\boldsymbol{h}_{BU}\\
&\quad+\left(\boldsymbol{f}^T(t)\otimes\mathbf{z}^H(t)\right)\left(\mathbf{A}_{UE}^{*}\otimes\mathbf{A}_{BS}\right)\left(\mathrm{vec}\left(\mathbf{A}_{RIS}^{H}\Phi\mathbf{A}_{RIS}\right)^T\otimes\boldsymbol{I}\right)\boldsymbol{h}_{BRU}+n(t).
\end{aligned} \tag{8}$$

where (a) is derived from

$$\begin{aligned}
\mathrm{vec}\left(\boldsymbol{H}_{BRU}\right)&=\mathrm{vec}\left(\mathbf{A}_{BS}\boldsymbol{H}_{\beta}\mathbf{A}_{RIS}^{H}\boldsymbol{\Phi}\mathbf{A}_{RIS}\boldsymbol{H}_{\delta}\mathbf{A}_{UE}^{H}\right)\\
&=\left(\mathbf{A}_{UE}^{*}\otimes\mathbf{A}_{BS}\right)\mathrm{vec}\left(\boldsymbol{H}_{\beta}\mathbf{A}_{RIS}^{H}\boldsymbol{\Phi}\mathbf{A}_{RIS}\boldsymbol{H}_{\delta}\right)\\
&=\left(\mathbf{A}_{UE}^{*}\otimes\mathbf{A}_{BS}\right)\left(\boldsymbol{H}_{\delta}^{T}\otimes\boldsymbol{H}_{\beta}\right)\mathrm{vec}\left(\mathbf{A}_{RIS}^{H}\boldsymbol{\Phi}\mathbf{A}_{RIS}\right)\\
&=\left(\mathbf{A}_{UE}^{*}\otimes\mathbf{A}_{BS}\right)\left(\mathrm{vec}\left(\mathbf{A}_{RIS}^{H}\Phi\mathbf{A}_{RIS}\right)^T\otimes\boldsymbol{I}\right)\mathrm{vec}\left(\boldsymbol{H}_{\delta}^{T}\otimes\boldsymbol{H}_{\beta}\right)
\end{aligned} \tag{9}$$

where $(\cdot)^*$ represents the complex conjugate operator, $\boldsymbol{h}_{BU}\triangleq\mathrm{vec}\left(\boldsymbol{H}_{\alpha}\right)$ and $\boldsymbol{h}_{BRU}\triangleq\mathrm{vec}\left(\boldsymbol{H}_{\delta}^{T}\otimes\boldsymbol{H}_{\beta}\right)$, $\otimes$ denotes the Kronecker product. By collecting all measurements $y(t)$, the corresponding signal are stacked into a vector form $\mathbf{y}\triangleq[\mathbf{y(1)},\ldots,\mathbf{y(T)}]^{\mathbf{T}}$, which can be expressed as

$$\begin{aligned}
\mathbf{y}&=\begin{bmatrix}\boldsymbol{f}^T(1)\otimes\mathbf{z}^H(1)\\ \vdots\\ \boldsymbol{f}^T(T)\otimes\mathbf{z}^H(T)\end{bmatrix}\left(\mathbf{A}_{UE}^{*}\otimes\mathbf{A}_{BS}\right)\boldsymbol{h}_{BU}\\
&\quad+\begin{bmatrix}\boldsymbol{f}^T(1)\otimes\mathbf{z}^H(1)\\ \vdots\\ \boldsymbol{f}^T(T)\otimes\mathbf{z}^H(T)\end{bmatrix}\left(\mathbf{A}_{UE}^{*}\otimes\mathbf{A}_{BS}\right)\left(\mathbf{A}_{RIS}^{T}\otimes\mathbf{A}_{RIS}^{H}\right)\boldsymbol{h}_{BRU}+\boldsymbol{n}\\
&=\boldsymbol{\Psi}_{BU}\boldsymbol{h}_{BU}+\boldsymbol{\Psi}_{BRU}\boldsymbol{h}_{BRU}+\boldsymbol{n}.
\end{aligned} \tag{10}$$

with

$$\boldsymbol{\Psi}_{BU}=\begin{bmatrix}\boldsymbol{f}^T(1)\otimes\mathbf{z}^H(1)\\ \vdots\\ \boldsymbol{f}^T(T)\otimes\mathbf{z}^H(T)\end{bmatrix}\left(\mathbf{A}_{UE}^{*}\otimes\mathbf{A}_{BS}\right) \tag{11}$$

$$\begin{aligned}
\boldsymbol{\Psi}_{BRU}&=\begin{bmatrix}\boldsymbol{f}^T(1)\otimes\mathbf{z}^H(1)\\ \vdots\\ \boldsymbol{f}^T(T)\otimes\mathbf{z}^H(T)\end{bmatrix}\left(\mathbf{A}_{UE}^{*}\otimes\mathbf{A}_{BS}\right)\\
&\quad\times\left(\boldsymbol{H}_{\delta}^{T}\otimes\boldsymbol{H}_{\beta}\right)\left(\mathbf{A}_{RIS}^{T}\otimes\mathbf{A}_{RIS}^{H}\right).
\end{aligned} \tag{12}$$

Since $\boldsymbol{h}_{BU}$ and $\boldsymbol{h}_{BRU}$ are sparse, the channel estimation problem based on (10) becomes a sparse recovery problem. The CS-based sparse signal recovery method has the potential to achieve a substantial training overhead reduction [9]. It follows that a high-dimensional sparse channel can be estimated by using the CS sparse recovery algorithm.

III. Channel Estimation

In this section, the paper will address the sparse representation framework of RIS-assisted channel estimation. The whole channel is decomposed into LOS-path and reflected-path. The LOS-path means the straight-line channel from BS to user, while the reflected-path means the channel signal is reflected by the RIS from BS to user.

A. Proposed RIS-Assisted Channel Estimation Framework

In this subsection, we will detailed introduce the sparse representation framework of RIS-assisted channel estimation. Based on the (10), we aim to estimate the LOS and reflected channel, simultaneously. In the proposed mmWave MIMO system, we can adjust the reflecting elements of RIS to change channel propagation environment. Two regularization terms are developed to improve the performance of channel estimation. The optimization problem can be formulated as

$$\min_{\boldsymbol{h},\boldsymbol{h}_{BU},\boldsymbol{h}_{BRU}} \frac{1}{2}\| \mathbf{y}-\boldsymbol{\Psi}\boldsymbol{h}\|_2^2+\mu_{BU}\mathbf{g}_{BU}\left(\boldsymbol{h}_{BU}\right)+\mu_{BRU}\mathbf{g}_{BRU}\left(\boldsymbol{h}_{BRU}\right), \quad (13)$$

where $\boldsymbol{\Psi}=\left[\boldsymbol{\Psi}_{BU}\boldsymbol{\Psi}_{BRU}\right]$ and $\boldsymbol{h}=\left[\boldsymbol{h}_{BU}^T\boldsymbol{h}_{BRU}^T\right]^T$, μ_{BU} and μ_{BRU} denote the regularization parameters, respectively. It is difficult to solve the nonconvex optimization problem (13), due to the multi-variables and coupling each other.

To solve this optimization problem, the received signal $\mathbf{y}_m$ is divided into $\mathbf{y}_{BU}$ and $\mathbf{y}_{BRU}$ by exploiting the linearity of LOS-path and reflected-path, respectively. Thus, letting $\mathbf{y}=\left[\mathbf{y}_{BU}^T\mathbf{y}_{BRU}^T\right]^T$, we introduce the auxiliary variable $\boldsymbol{u}$ to reformulate the optimization problem (13) as

$$\begin{aligned}&\min_{\boldsymbol{h},\boldsymbol{h}_{BU},\boldsymbol{h}_{BRU}} \frac{1}{2}\left\|\mathbf{y}_{BU}-\boldsymbol{\Psi}_{BU}\boldsymbol{h}_{BU}\right\|_2^2+\mu_{BU}\mathbf{g}_{BU}\left(\boldsymbol{h}_{BU}\right)\\ &+\frac{1}{2}\left\|\mathbf{y}_{BRU}-\boldsymbol{\Psi}_{BRU}\boldsymbol{h}_{BRU}\right\|_2^2+\mu_{BRU}\mathbf{g}_{BRU}\left(\boldsymbol{h}_{BRU}\right)+\frac{\kappa}{2}\| \boldsymbol{h}-\boldsymbol{u}\|_2^2 \quad (14)\\ &\text{s.t.} \quad \boldsymbol{u}=\boldsymbol{h}_{BU}+\boldsymbol{h}_{BRU}.\end{aligned}$$

It follows that the optimization problem (14) includes three variables, which can be solved by the alternative optimization scheme. Then, we introduce an alternating direction iterative framework to determine the LOS-path and reflected-path channels.

B. LOS Channel Estimation

In this subsection, the LOS channel is estimated by exploiting the weighted ℓ_1-norm regularization model. To this end, the LOS channel $\boldsymbol{h}_{BU}$ is optimized by fitting the $\boldsymbol{h}_{BRU}$ as follows

$$\min_{\boldsymbol{h}_{BU}} \frac{1}{2}\left\|\mathbf{y}_{BU}-\boldsymbol{\Psi}_{BU}\boldsymbol{h}_{BU}\right\|_2^2+\mu_{BU}\mathbf{g}_{BU}\left(\boldsymbol{h}_{BU}\right), \quad (15)$$

where $\mathbf{y}_{BU}=\mathbf{y}-\boldsymbol{\Psi}_{BRU}\boldsymbol{h}_{BRU}$, $\mu_{BU}>0$ denotes a regularization parameter. Specifically, let's set $\boldsymbol{h}_{BRU}=\mathbf{0}$ at the beginning. For the LOS channel, we utilize a weighted ℓ_1-norm regularization to characterize the LOS-path channel information, which can be expressed as

$$\mathbf{g}_{BU}\left(\boldsymbol{h}_{BU}\right)=\mu_{BU}\sum_{i=1}^{L_{BU}} w(i)\left|h_{BU}(i)\right|, \quad (16)$$

where $h_{BU}(i)$ is the i-th element of channel $\boldsymbol{h}_{BU}$. $w(i)$ is the i-th of the weight, which can ensure the denominator not less than zero.

By exploiting the weighted ℓ_1-norm regularization (16), the optimization problem (15) is rewritten as

$$\min_{\boldsymbol{h}_{BU}} \frac{1}{2}\left\|\mathbf{y}_{BU}-\boldsymbol{\Psi}_{BU}\boldsymbol{h}_{BU}\right\|_2^2+\mu_{BU}\sum_{i=1}^{L_{BU}} w(i)\left|h_{BU}(i)\right|. \quad (17)$$

Solving (17) directly will incur huge complexity. To address this issue, the iterative shrinkage thresholding algorithm is utilized. We construct a quadratic formula as

$$\min_{\boldsymbol{h}_{BU}} \frac{1}{2t}\left\|\boldsymbol{h}_{BU}^{(k)}+t\boldsymbol{\Psi}^T\left(\mathbf{y}_{BU}-\boldsymbol{\Psi}_{BU}\boldsymbol{h}_{BU}^{(k)}\right)-\boldsymbol{h}_{BU}^{(k+1)}\right\|_2^2+D, \quad (18)$$

where t is step size and D is a constant. It is observed that the solution of problem (18) is close to the optimal solution of (17), accompanied by a substantial reduction in the complexity. The zero point of problem (18) can be given by

$$\boldsymbol{h}_{BU}^{(k+1)}=\boldsymbol{S}\left(\boldsymbol{h}_{BU}^{(k)}+t\boldsymbol{\Psi}^T\left(\mathbf{y}_{BU}-\boldsymbol{\Psi}_{BU}\boldsymbol{h}_{BU}^{(k)}\right)\right). \quad (19)$$

To improve iteration speed and estimation accuracy, the soft thresholding algorithm is used in (19), which can be expressed as

$$\boldsymbol{S}_{BU}(i)=\operatorname{sign}\left(\boldsymbol{h}_{BU}^{(k)}\right)\left|\,|\boldsymbol{h}_{BU}|-\frac{\mu_{BU}}{t}w(i)\right|, \quad (20)$$

where $\frac{\mu_{BU}}{t}$ is thresholding value that plays a role in controlling the step size of each iteration.

C. Reflected Channel Estimation

After the completion of LOS channel estimation, it needs further to solve the reflected channel estimation by fitting the LOS channel $\boldsymbol{h}_{BU}$. Then, the solution to the problem (14) with respect to $\boldsymbol{h}_{BRU}$ can be rewritten as

$$\min_{\boldsymbol{h}_{BRU}} \frac{1}{2}\left\|\mathbf{y}_{BRU} - \boldsymbol{\Psi}_{BRU}\boldsymbol{h}_{BRU}\right\|_2^2 + \mu_{BRU}\mathbf{g}\left(\boldsymbol{h}_{BRU}\right), \tag{21}$$

where $\mathbf{y}_{BRU} = \mathbf{y} - \boldsymbol{\Psi}_{BU}\boldsymbol{h}_{BU}$.

To achieve precise performance, a robust $\ell_{1,\tau}$-norm is utilized to estimate the reflected channel by adjusting the parameter τ. Different τ may lead to different solution. However, the parameter τ is difficult to adjust due to $\ell_{1,\tau}$-norm model is non-convex. Therefore, it is important to determine the optimal value of parameter τ, and an adaptive parameter τ is considered in this paper. Based on this, the robust $\ell_{1,\tau}$ regularization function is utilized, which can be expressed as follows

$$\mathbf{g}\left(\boldsymbol{h}_{BRU}\right) = \frac{1}{\tau}\sum_{i=1}^{L_{BR}} \log\left(\cosh\left(\tau \boldsymbol{h}_{BRU}(i)\right)\right). \tag{22}$$

It is evident that (22) is exploited in the problem (21), which may lead to the nonconvex optimization problem. To address this issue, we utilize the first-order Taylor expansion to approximate $Q\left(\boldsymbol{h}_{BRU}\right)$. Let $Q\left(\boldsymbol{h}_{BRU}\right) = \log\left(\cosh\left(\tau\boldsymbol{h}_{BRU}\right)\right)$, which can be given by

$$Q\left(\boldsymbol{h}_{BRU}\right) = Q\left(\boldsymbol{h}_{BRU}^{(k)}\right) + \left\langle \nabla Q\left(\boldsymbol{h}_{BRU}^{(k)}\right), \boldsymbol{h}_{BRU} - \boldsymbol{h}_{BRU}^{(k)}, \right\rangle \tag{23}$$

where $Q\left(\boldsymbol{h}_{BRU}^{(k)}\right)$ is the k^{th} iteration of the solution. By removing the constants, the derivative of (23) can be formulated as

$$Q^{'}\left(\boldsymbol{h}_{BRU}\right) = \mu_n\left\langle \nabla \tanh\left(\tau\boldsymbol{h}_{BRU}^{(k)}\right), \boldsymbol{h}_{BRU}\right\rangle, \tag{24}$$

which may lead to the problem (21) rewritten as

$$\min_{\boldsymbol{h}_{BRU}} \frac{1}{2}\left\|\mathbf{y}_{BRU} - \boldsymbol{\Psi}_{BRU}\boldsymbol{h}_{BRU}\right\|_2^2 + \mu_n\left\langle \nabla \tanh\left(\tau\boldsymbol{h}_{BRU}^{(k)}\right), \boldsymbol{h}_{BRU}\right\rangle, \tag{25}$$

By utilizing the Karush-Kuhn-Tucher (KKT) condition, the solution of the problem (25) can be given by

$$\boldsymbol{h}_{BRU}^{(k+1)} = \left(\boldsymbol{\Psi}_{BRU}^{H}\boldsymbol{\Psi}_{BRU}\right)^{-1}\left(\boldsymbol{\Psi}_{BRU}^{H}\mathbf{y}^{(k)} + \mu_{BRU}\tanh\left(\tau\boldsymbol{h}_{BRU}^{(k)}\right)\right). \tag{26}$$

It follows that channels $\boldsymbol{h}_{BU}$ and $\boldsymbol{h}_{BRU}$ can be optimized by solving the alternate optimization problems (13) and (21).

D. Parameter τ Updating

As we can see that the choosing of τ directly affects the ability of regularization term. To reduce the artificial error, the parameter τ is updated in every iteration. The problem in (21) can be written as

$$\min_{\boldsymbol{h}_{BRU}} \frac{1}{2}\left\|\mathbf{y}_{BRU} - \boldsymbol{\Psi}_{BRU}\boldsymbol{h}_{BRU}\right\|_2^2 + \mu_{BRU}\log\left(\cosh\left(\tau\boldsymbol{h}_{BRU}\right)\right). \tag{27}$$

It is not difficult to observe that the optimization problem is general convex constrained quadratic programs whose optimal solution can be obtained by exploiting KKT condition. That is

$$\tau^{(k)}\boldsymbol{h}_{BRU}^{(k)} = \operatorname{arctanh}\left(\frac{1}{\mu_{BRU}}\boldsymbol{\Psi}_{BRU}^{H}\left(\boldsymbol{\Psi}_{BRU}\boldsymbol{h}_{BRU} - \boldsymbol{y}_{BRU}^{(k)}\right)\right). \tag{28}$$

After taking ℓ_2-norm at both sides of (28), the corresponding solution of the parameter $\tau^{(k)}$ can be rewritten as

$$\tau^{(k)} = \frac{\left\|\operatorname{arctanh}\left(\frac{1}{\mu_{BRU}}\boldsymbol{\Psi}_{BRU}^{H}\left(\boldsymbol{\Psi}_{BRU}\boldsymbol{h}_{BRU} - \boldsymbol{y}_{BRU}^{(k)}\right)\right)\right\|_2}{\left\|\boldsymbol{h}_{BRU}^{(k)}\right\|_2 + \eta}, \tag{29}$$

where a small constant η is provided to avoid the denominator close to zero. It follows that the parameter τ can be updated in each iteration.

E. Hybrid Channel Updating

After the LOS channel $\boldsymbol{h}_{BU}$ and the reflected channel $\boldsymbol{h}_{BRU}$ are estimated, the following optimization channel model is developed to characterize the mmWave channel, which can be formulated as

$$\min_{\boldsymbol{h}} \frac{1}{2}\|\mathbf{y} - \boldsymbol{\Psi}\boldsymbol{h}\|_2^2 + \frac{\kappa}{2}\|\boldsymbol{h} - \boldsymbol{u}\|_2^2. \tag{30}$$

It is obvious that above optimization problem (30) is a convex problem. By utilizing the Karush-Kuhn-Tucher (KKT) condition, we have

$$\boldsymbol{h} = \left(\boldsymbol{\Psi}^{H}\boldsymbol{\Psi} + \kappa\boldsymbol{I}\right)^{-1}\left(\boldsymbol{\Psi}^{H}\mathbf{y} + \kappa\boldsymbol{u}\right) \tag{31}$$

Through this three-stage scheme, the channels $\boldsymbol{h}_{BU}$, $\boldsymbol{h}_{BRU}$ and $\boldsymbol{h}$ can be effectively decoupled and provides better results. As a consequence, the proposed three-stage scheme is illustrated in Algorithm 1.

Algorithm 1 Parallel channel estimation algorithm

1: **Input:** Given the measurements $\mathbf{y}$, and the matrices $\boldsymbol{\Psi}_{BRU}$, $\boldsymbol{\Psi}_{BU}$

2: **Initialization:** $\mathcal{K} = \{1, 2, \ldots, K\}$, $\boldsymbol{h}_{BRU} = \mathbf{0}$;

3: Update $\mathbf{y}_{BU}$ with $\mathbf{y}_{BU} = \mathbf{y} - \boldsymbol{\Psi}_{BRU}\boldsymbol{h}_{BRU}$;

4: **1. Estimate $\boldsymbol{h}_{BU}$ by solving**

$$\min_{h_{BU}} \frac{1}{2}\left\|\mathbf{y}_{BU} - \mathbf{\Psi}_{BU}\boldsymbol{h}_{BU}\right\|_2^2 + \mu_{BU}\mathbf{g}_{BU}\left(\boldsymbol{h}_{BU}\right);$$

Update $\mathbf{y}_{BRU}$ with $\mathbf{y}_{BRU} = \mathbf{y} - \mathbf{\Psi}_{BU}\boldsymbol{h}_{BU}$;

2. Estimate $\boldsymbol{h}_{BRU}$ by solving

$$\min_{h_{BRU}} \frac{1}{2}\left\|\mathbf{y}_{BRU} - \mathbf{\Psi}_{BRU}\boldsymbol{h}_{BRU}\right\|_2^2 + \mu_{BRU}\mathbf{g}_{BRU}\left(\boldsymbol{h}_{BRU}\right);$$

Update $\boldsymbol{u}$ with $\boldsymbol{u} = \boldsymbol{h}_{BU} + \boldsymbol{h}_{BRU}$;

3. Estimate $\boldsymbol{h}$ by solving

$$\min_{h} \frac{1}{2}\left\|\mathbf{y} - \mathbf{\Psi}\boldsymbol{h}\right\|_2^2 + \frac{\mathcal{K}}{2}\left\|\boldsymbol{h} - \boldsymbol{u}\right\|_2^2;$$

end

Output $\boldsymbol{h}_{BU}$, $\boldsymbol{h}_{BRU}$, $\boldsymbol{h}$.

IV. Simulation Results

In this section, experiments are carried out to demonstrate the effectiveness of the proposed algorithm. As the RIS is practically deployed with the 8×8 planar antenna array to enhance the communication link. The system bandwidth and carrier frequency were set to 20MHz and 2GHz, respectively. The simulation parameters are set as $N_{UE} = 6$ and $N_t = 128$. Due to the limited downlink pilot resources, we consider reflecting elements $N_{RIS} = 16, 32, 64$, respectively. To quantify the estimator performance, the average normalized MSE between the estimated and the original channel are calculated through Monte Carlo methods, which is averaged over channel realizations. The corresponding normalized MSE is defined as

$$\mathrm{NMSE} = \frac{\left\|\boldsymbol{h} - \hat{\boldsymbol{h}}\right\|_2^2}{\left\|\boldsymbol{h}\right\|_2^2} \tag{32}$$

where $\boldsymbol{h}$ and $\hat{\boldsymbol{h}}$ are the original and estimated channels, respectively.

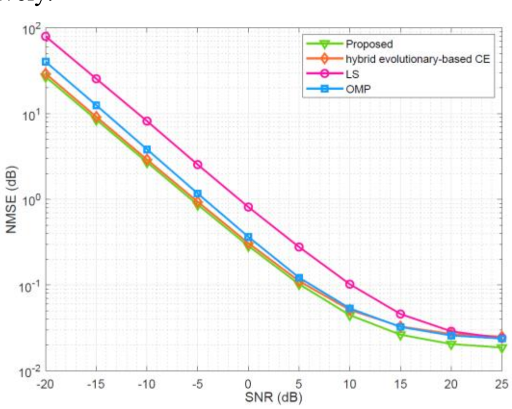

Fig. 2. NMSE performance of the proposed channel estimator versus the SNRs in dB.

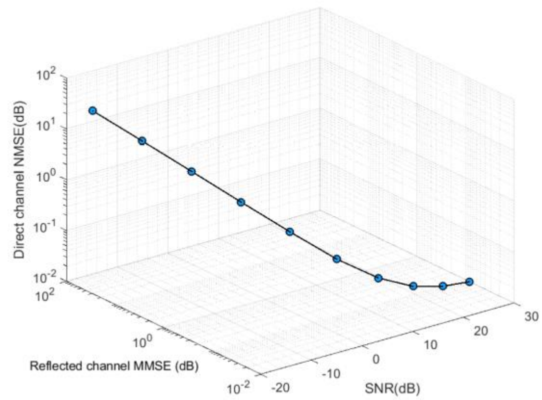

Fig. 3. NMSE performance comparisons between LOS and reflected channel estimation.

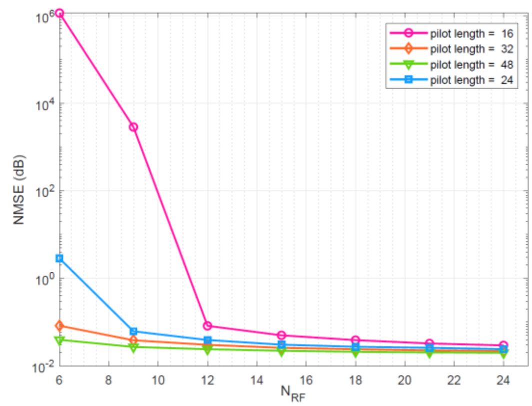

Fig. 4. NMSE performance of the proposed channel estimator versus the number of RF chain.

The proposed channel estimator is compared with conventional schemes, such as the LS, OMP and hybrid evolutionary based channel estimator. As observed from Fig. 2, the simulation results are observed that the proposed estimator keep consistent with the theoretical curves along with the increase of SNR. Meanwhile, as the SNR level increases, the MSEs for all those estimators decrease and gradually reach stable. This favorable result can be attributed to the fact that when SNR level is low, the effect of noise gives a dominant influence on the performance of channel estimation. It is acknowledged that LS estimator is vulnerable to noise, this conclusion also is validated in our simulations that the LS estimator performs poorly in a low SNR level. That is to say, the proposed scheme is more robust than LS. OMP estimator reaches the similar performance to the LS estimator without prior knowledge of CSI. The simulation result show that whenever the SNR value is small or large, the proposed algorithm always achieves clearly performance improvement compared with the LS and OMP estimators, which verifies that the proposed scheme can well applied to the different SNR levels.

In addition, the hybrid evolutionary-based channel estimator also is employed for comparison. Simulation results confirm that the proposed joint sparse estimator is a best solution under the RIS-assisted channel. It is important to point that the effect of noise can be almost ignored in the high SNR zone, and hence it can be seen that three estimators converge to the stable state, when the SNR levels are not lower than 20.

In Figs. 3, the simulated NMSE of the channel estimation approach for the LOS and reflected channels, where the SNR levels from -20dB and 30dB are taken into the numerical experiments. It is observed that the NMSEs of LOS and reflected channels decrease significantly with the SNR level increasing. This is because the proposed algorithm utilizes the weighted ℓ_1 -norm and robust $\ell_{1,r}$ -norm to improve the estimation accuracy. From this results, we observe that the LOS and reflected channels both offer promising performance in the NMSE. This will attract great attention in the application of RIS to the existing IoT system to boost the channel estimation process.

Finally, the pilot contamination performance is investigated to verify the robustness of the proposed estimator for different pilot length and radio frequency (RF) chains. All simulation results are obtained in Fig. 4. It is obvious that there exists an increasing NMSE performance loss when the number of pilots reducing. These results verify the effectiveness of the proposed estimator. However, the performance of the proposed channel estimator is almost unaffected by the high SNR levels. This is because that the effect of noise can be almost ignored in the high SNR zone, and hence our findings show that the three estimators appears to have the best performance in term of NMSE values.

V. Conclusion

In this paper, we investigated the problem of sparse channel estimator for the RIS-assisted IoT system using merely a small number of pilot symbols. Under the proposed framework, the weighted ℓ_1 norm minimization and ℓ_1 norm minimization criterion have been utilized to efficiently perform super-resolution channel parameter estimation, respectively. To solve this non-convex sparse recovery problem, we utilized the alternating direction algorithm to estimate the channel with a few pilot symbols. Simulation results confirmed the desirable performance of the proposed scheme compared to the LS, OMP and hybrid evolutionary-based channel estimation, as it works for RIS-assisted communication scenarios. Moreover, it would be interesting to observe that the number of RIS unit elements and the RF chain has significant effect on the performance of the proposed estimator.

References

[1] J. Wang, G. Wang, B. Li, H. Yang, Y. Hu, and A. Schmeink, “Massive mimo two-way relaying systems with swipt in iot networks,” IEEE Internet of Things Journal, vol. 8, no. 20, pp. 15 126–15 139, 2021.

[2] Z. Chen, X. Du, J. Tang, X. Y. Zhang, and K.-K. Wong, “Joint Location and Channel Error Optimization for Beamforming Design for Multi-RIS Assisted MIMO System,” IEEE SAM 2022, pp. 53–59.

[3] C. You, B. Zheng, and R. Zhang, “Wireless communication via double irs: Channel estimation and passive beamforming designs,” IEEE Wireless Communications Letters, vol. 10, no. 2, pp. 431–435, 2021.

[4] S. Sun and H. Yan, “Channel estimation for reconfigurable intelligent surface-assisted wireless communications considering doppler effect,” IEEE Wireless Communications Letters, vol. 10, no. 4, pp. 790–794, 2021.

[5] Z. Chen, J. Tang, X. Y. Zhang, D. K. C. So, S. Jin, and K.-K. Wong, “Hybrid evolutionary-based sparse channel estimation for irs-assisted mmwave mimo systems,” IEEE Transactions on Wireless Communications, vol. 21, no. 3, pp. 1586–1601, 2022.

[6] Y. Gao, J. Xu, W. Xu, D. W. K. Ng, and M.-S. Alouini, “Distributed irs with statistical passive beamforming for miso communications,” IEEE Wireless Communications Letters, vol. 10, no. 2, pp. 221–225, 2021.

[7] J. Mirza and B. Ali, “Channel estimation method and phase shift design for reconfigurable intelligent surface assisted mimo networks,” IEEE Transactions on Cognitive Communications and Networking, vol. 7, no. 2, pp. 441–451, 2021.

[8] P. Wang, J. Fang, H. Duan, and H. Li, “Compressed channel estimation for intelligent reflecting surface-assisted millimeter wave systems,” IEEE Signal Processing Letters, vol. 27, pp. 905–909, 2020.

[9] Z. Chen, J. Tang, H. Tang, X. Zhang, D. K. C. So, and K.-K. Wong, “Channel estimation of irs-aided communication systems with hybrid multiobjective optimization,” in ICC 2021 - IEEE International Conference on Communications, 2021, pp. 1–6.

[10] Z. Chen, J. Tang, X. Y. Zhang, Q. Wu, Y. Wang, D. K. C. So, S. Jin, and K.-K. Wong, “Offset learning based channel estimation for intelligent reflecting surface-assisted indoor communication,” IEEE Journal of Selected Topics in Signal Processing, vol. 16, no. 1, pp. 41–55, 2022.

[11] C. Liu, X. Liu, D. W. K. Ng, and J. Yuan, “Deep residual learning for channel estimation in intelligent reflecting surface-assisted multiuser communications,” IEEE Transactions on Wireless Communications, vol. 21, no. 2, pp. 898–912, 2022.

[12] A. Alkhateeb, O. El Ayach, G. Leus, and R. W. Heath, “Channel estimation and hybrid precoding for millimeter wave cellular systems,” IEEE Journal of Selected Topics in Signal Processing, vol. 8, no. 5, pp. 831–846, 2014.